

Equation of state for polymer liquid crystals: Theory and experiment

H. H. Strey,^{*} V. A. Parsegian, and R. Podgornik[†]

National Institutes of Health, National Institute of Child Health and Human Development, Laboratory of Physical and Structural Biology, Building 12A/2041, Bethesda, Maryland 20892-5626

(Received 2 March 1998)

The first part of this paper develops a theory for the free energy of lyotropic polymer nematic liquid crystals. We use a continuum model with macroscopic elastic moduli for a polymer nematic phase. By evaluating the partition function, considering only harmonic fluctuations, we derive an expression for the free energy of the system. We find that the configurational entropic part of the free energy enhances the effective repulsive interactions between the chains. This configurational contribution goes as the fourth root of the direct interactions. Enhancement originates from the coupling between bending fluctuations and the compressibility of the nematic array normal to the average director. In the second part of the paper we use osmotic stress to measure the equation of state for DNA liquid crystals in 0.1M to 1M NaCl solutions. These measurements cover five orders of magnitude in DNA osmotic pressure. At high osmotic pressures the equation of state, dominated by exponentially decaying hydration repulsion, is independent of the ionic strength. At lower pressures the equation of state is dominated by fluctuation enhanced electrostatic double layer repulsion. The measured equation of state for DNA fits well with our theory for all salt concentrations. We are able to extract the strength of the direct electrostatic double layer repulsion. This is an alternative way of measuring effective charge densities along semiflexible polyelectrolytes. [S1063-651X(99)11401-6]

PACS number(s): 87.15.Nn, 61.30.-v, 64.30.+t

I. INTRODUCTION

In biology, there exists a class of bulk materials that provides the cell's structural stability and ensures its integrity in multicell environments. These materials are often made from biopolymers with varying intrinsic stiffness and helicity such as actin, fibrin, collagen, polysaccharides, elastin, tubulin. In most cases biology controls elastic properties by controlled polymerization and depolymerization of the monomers and by enzymatically controlled crosslinking of polymer strands. Often biopolymers, because of their intrinsic stiffness, form liquid crystals at *in vivo* concentrations. Because these polymers are mechanically uniform, their phase behavior is predominantly determined by the volume fraction of the polymer in its solvent, rather than by temperature. Such materials are called lyotropic systems. In contrast, polymeric liquid crystalline materials used in industrial applications (like main-chain and side-chain polymer liquid crystals) are most often thermotropic, because of their flexible backbones. Thermotropic means that temperature determines their phase behavior.

Biopolymer materials are interesting for several reasons. First of all, there are many biomaterials made from or with biopolymers exhibiting mechanical properties unreached by most conventional synthetic materials, whether the focus is strength, flexibility, or a combination of both. Needless to

say, little is understood about their design, structure, and how they work. There is also the increasingly appreciated potential of biopolymers for basic material and condensed matter research [1]. In most synthetic polymer systems it is extremely difficult to control properties of individual polymers, like their degree of polymerization, crosslinks, and chemical uniformity. By using modern molecular biological and biochemical techniques it is possible to tailor biopolymers almost at will, using nature's own efficient polymerization machinery. So it is, for example, possible to prepare monodisperse DNA fragment solutions with lengths varying from a few nm to several μm using recombinant DNA methodology. This is not yet possible with any other polymer.

DNA liquid crystals are also of immediate interest, because they model packing of DNA in confined spaces, as in cell nuclei and viral phage heads (see, e.g., [2-4]). Moreover, it is believed that packing of DNA in chromatin plays an important role in gene regulation [5]. By understanding how much energy is needed to compact DNA we will gain insight into these processes as well.

One of the questions in condensed matter physics is how to relate microscopic interactions to condensed state bulk properties, like elastic and dielectric constants, heat capacity, and packing symmetries. In an experiment we can go the other way. The question is then, can we infer microscopic interactions from macroscopic behavior?

In this paper we explore the equation of state for DNA liquid crystals [6] using the osmotic stress method [7]. It allows us to control all intensive variables of the system, namely, the chemical potentials of both water and salt. According to the Gibbs-phase rule, this leaves us, after equilibration against solutions of known activities, with a single phase. The absence of phase coexistence is crucial for determining the structure of the different phases using x-ray scat-

^{*}Permanent address: Department of Polymer Science and Engineering, University of Massachusetts—Amherst, Amherst, MA 01003.

[†]On leave from Department of Physics, Faculty of Mathematics and Physics, University of Ljubljana and Department of Theoretical Physics, "J. Stefan" Institute, Ljubljana, Slovenia.

tering. At the same time the osmotic stress method provides us with information about the free energy of the system, which can be obtained by integrating the equation of state (osmotic pressure Π versus DNA density).

The ability to measure an equation of state and to map the phase diagram for free energies made us realize that there was no polymer liquid crystalline theory for free energies. This is not surprising considering that typical liquid crystalline theories are continuum elastic theories expanding deformations around the symmetries of the system. Because these approaches are only good for long-wavelength physics, it is very hard to use them to predict free energies.

Despite these difficulties, we will show in the first part of this paper that in our particular case with exponential interactions between the polymer chains, the free energy can be derived starting from a macroscopic theory. The microscopic interactions were incorporated into the continuum elastic moduli: the three Frank constants K_1 , K_2 , K_3 and the bulk compressibility perpendicular to the chains \mathcal{B} . By evaluating the partition function, considering only harmonic fluctuations, we derive an expression for the free energy of the system. To make the free energy finite we had to introduce a short-wavelength cutoff. We argue that the form of the free energy is robust, meaning that the free energy behavior with respect to density does not strongly depend on the particular choice of cutoff.

We find that the fluctuation part of the free energy, going as the fourth root of the direct interactions, enhances the repulsive interactions between the chains. Enhancement originates from coupling between bending fluctuations and the compressibility of the nematic array normal to the average director. The results should be applicable to lyotropic polymer liquid crystals with fluidlike positional order like nematics or hexatics. We think that it even can be applied to chiral phases, like cholesterics and blue phases. In typical chiral phases the twist extends over several hundred intermolecular spacings, so that in these phases local parallel packing can still be used.

We compare theoretical predictions with measurements of equations of state for DNA liquid crystals under different ionic conditions over almost five orders of magnitude in osmotic pressure [6]. By extracting the form of the fluctuation part of the measured free energy and assuming exponentially decaying repulsive interactions (screened electrostatic and hydration) between DNA molecules, we have been able to extract the strength of the direct electrostatic double layer repulsion. This extraction creates an alternative way of directly measuring effective charge densities along semiflexible polyelectrolytes.

II. POLYMER NEMATIC THEORY

Let us first consider the elastic free energy of a nematic: a three-dimensional liquid with long-range orientational order and an average director \mathbf{n} along the z axis. Such phases are typically formed by solutions of rodlike or disklike objects. There are three kinds of deformations in quadratic order of \mathbf{n} with symmetry $C_{\infty h}$: splay, twist, and bending. The corresponding elastic constants for these deformations are the Frank constants K_1 (splay), K_2 (twist), and K_3 (bend).

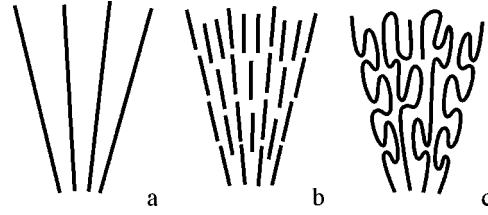


FIG. 1. Illustration of how splay couples to the density of different nematic liquid crystals: (a) stiff, long rods; (b) stiff, short rods; (c) semiflexible, long polymers. Long, stiff rods (a) show strong density changes when splayed. In the case of short and stiff rods (b) the voids created by splaying the material are filled by other short rods. For long, semiflexible polymers (c) the voids are filled by polymers folding back on themselves.

$$\mathcal{F}_N = \frac{1}{2} \int d^2 \mathbf{r}_\perp dr_z \{ K_1 (\nabla \cdot \mathbf{n})^2 + K_2 [\mathbf{n} \cdot (\nabla \times \mathbf{n})]^2 + K_3 [\mathbf{n} \times (\nabla \times \mathbf{n})]^2 \}. \quad (1)$$

For small deviations of the director field $\mathbf{n}(\mathbf{r})$ around its average orientation along the z axis $\mathbf{n}(\mathbf{r}) \approx (\delta n_x(\mathbf{r}), \delta n_y(\mathbf{r}), 1)$, the free energy assumes the form

$$\mathcal{F}_N = \frac{1}{2} \int d^2 \mathbf{r}_\perp dz [K_1 (\nabla_\perp \cdot \delta \mathbf{n})^2 + K_2 (\nabla_\perp \times \delta \mathbf{n})^2 + K_3 (\partial_z \delta \mathbf{n})^2]. \quad (2)$$

For polymer nematics we now have to consider that the director field $\mathbf{n}(\mathbf{r})$ and the densities of polymers in the (x, y) plane $\rho = \rho_0 + \delta \rho$ are coupled [8,9]. If the polymers were infinitely long and stiff the coupling is given by the continuity equation:

$$\partial_z \delta \rho + \rho_0 \nabla_\perp \cdot \delta \mathbf{n} = 0. \quad (3)$$

We assume [10] that this constraint applies along a certain typical length of the polymer l , which should be on the order of the persistence length \mathcal{L}_p . On length scales much larger than l the polymer can either fill the voids with its own ends or fold back on itself [11], both effects leading to violation of the constraint Eq. (3). On these length scales the polymer nematic can splay without density change as illustrated in Fig. 1. Following [12,13] this can be expressed by introducing G , a measure of how effectively the constraint is enforced. Density changes are expanded to second order in density deviations $\delta \rho(\mathbf{r}_\perp, z) = \rho(\mathbf{r}_\perp, z) - \rho_0$. \mathcal{B} is the bulk modulus for compressions and dilations normal to the chains. The total mesoscopic Hamiltonian (\mathcal{H}) can be written

$$\mathcal{H} = \mathcal{F}_0(\rho_0) + \frac{1}{2} \int d^2 \mathbf{r}_\perp dz \times \left[\mathcal{B} \left(\frac{\delta \rho}{\rho_0} \right)^2 + G (\partial_z \delta \rho + \rho_0 \nabla_\perp \cdot \delta \mathbf{n})^2 \right] + \mathcal{F}_N, \quad (4)$$

where G is given by

$$G = \frac{k_B T l}{2 \rho_0}. \quad (5)$$

The form of the coupling constant G can be obtained from the observation that $\partial_z \delta \rho + \rho_0 \nabla_\perp \cdot \delta \mathbf{n}$ equals the local difference between the number of chain heads and tails [9]. From here one derives that G is the concentration susceptibility for an ideal mixture of heads and tails, thus

$$G = \frac{k_B T}{(\rho_H + \rho_T)}, \quad (6)$$

where ρ_H and ρ_T are the average concentrations of heads and tails, with $\rho_H, \rho_T = \rho_{\text{chain}}$. The chain density, on the other hand, equals $\rho_{\text{chain}} = \rho_0 / l$, wherefrom $G = k_B T l / 2 \rho_0$. The corresponding structure factor can be written as [13]

$$\begin{aligned} \mathcal{S}(q_\perp, q_z) &= \langle |\delta \rho(q_\perp, q_z)|^2 \rangle \\ &= k_B T \frac{\rho_0^2 q_\perp^2 + k_B T \mathcal{K}(\mathbf{q}) / G}{\mathcal{B} q_\perp^2 + k_B T (\mathcal{B} / G \rho_0^2 + q_z^2) \mathcal{K}(\mathbf{q})}, \end{aligned} \quad (7)$$

where we defined

$$\mathcal{K}(\mathbf{q}) = \frac{K_1 q_\perp^2 + K_3 q_z^2}{k_B T}. \quad (8)$$

For stiff polymer chains like DNA the limit $G \rightarrow \infty$ is appropriate, leading to the structure factor proposed by Selinger and Bruinsma [14],

$$\mathcal{S}(q_\perp, q_z) = k_B T \frac{\rho_0^2 q_\perp^2}{K_1 q_\perp^2 q_z^2 + K_3 q_z^4 + \mathcal{B} q_\perp^2}. \quad (9)$$

In order to calculate the contribution to the free energy due to fluctuations in nematic order we first have to sum over all the density modes. From here on we will consider only fluctuations that are coupled to density changes. Because we are interested in how the free energy changes with density only those fluctuations will contribute. Twist deformations do not couple to density variations and can therefore be neglected. The trace over nematic director and density modes gives the free energy in the form

$$\mathcal{F} = \frac{1}{2} k_B T \int \int \frac{d^2 q_\perp dq_z}{(2\pi)^3} \ln(K_1 q_\perp^2 q_z^2 + K_3 q_z^4 + \mathcal{B} q_\perp^2). \quad (10)$$

To evaluate the integral, we take the partial derivative with respect to the compressibility \mathcal{B} ,

$$\frac{\partial \mathcal{F}}{\partial \mathcal{B}} = \frac{1}{2} k_B T V \int \int \frac{q_\perp dq_\perp dq_z}{(2\pi)^2} \frac{q_\perp^2}{K_1 q_\perp^2 q_z^2 + K_3 q_z^4 + \mathcal{B} q_\perp^2}. \quad (11)$$

The q_z integral can be done straightforwardly and we remain with

$$\frac{\partial \mathcal{F}}{\partial \mathcal{B}} = \frac{1}{2} k_B T \frac{V}{(2\pi)^2} \frac{\pi}{2} \int \frac{q_\perp^3 dq_\perp}{\sqrt{\mathcal{B} q_\perp^2} \sqrt{K_1 q_\perp^2 + 2\sqrt{\mathcal{B} K_3} q_\perp^2}}. \quad (12)$$

This integral depends essentially on the upper cutoff for $q_\perp = q_{\perp \text{max}}$ and we obtain

$$\frac{\partial \mathcal{F}}{\partial \mathcal{B}} = k_B T \frac{V}{4\pi} \frac{\mathcal{B} K_3}{K_1^2 \sqrt{\mathcal{B} K_1}} F\left(\frac{q_{\perp \text{max}}}{2\sqrt{\mathcal{B} K_3 / K_1^2}}\right), \quad (13)$$

where the function $F(x)$ has been defined as

$$\begin{aligned} F(x) &= \int_0^x \frac{u^{3/2} du}{\sqrt{1+u}} = \frac{1}{4} [\sqrt{x} \sqrt{1+x} (2x-3) + 3 \sinh^{-1} \sqrt{x}] \\ &= \begin{cases} \frac{2}{5} x^{5/2}, & x \ll 1 \\ \frac{1}{2} x^2, & x \gg 1. \end{cases} \end{aligned} \quad (14)$$

From here we obtain the two limiting forms of the free energy as

$$\mathcal{F} \approx \begin{cases} \frac{k_B T V}{5 \times 2^{3/2} \pi} \sqrt[4]{\frac{\mathcal{B}}{K_3}} q_{\perp \text{max}}^{5/2} + \dots, & q_{\perp \text{max}} \ll 2 \sqrt{\frac{\mathcal{B} K_3}{K_1^2}} \\ \frac{k_B T V}{16\pi} \sqrt{\frac{\mathcal{B}}{K_1}} q_{\perp \text{max}}^2 + \dots, & q_{\perp \text{max}} \gg 2 \sqrt{\frac{\mathcal{B} K_3}{K_1^2}}. \end{cases} \quad (15)$$

$$\quad (16)$$

Obviously the long-wavelength dependent physics is very complicated and depends crucially on the values of typical polymer length and the ratios of elastic constants. However, it depends also on the q_\perp cutoff. We have either to eliminate the cutoff by including higher order terms in the original Hamiltonian or to choose a meaningful cutoff. Higher order terms will capture the short-wavelength physics and remove the divergence.

In the following paragraph we want to show how this can be done for the low density limit Eq. (15). We are aware that in a more thorough treatment one has to include all possible higher order terms, but for right now we only include terms that will make integral Eq. (12) convergent. Letting $\mathcal{B} = \mathcal{B}(q_z, q_\perp)$, $K_3 = K_3(q_z, q_\perp)$, $K_1 = K_1(q_z, q_\perp)$, and taking into account the symmetry of the elastic nematic free energy, one can easily show that in order to make the integral in Eq. (12) converge in the low density limit Eq. (15), it is only necessary to expand \mathcal{B} as

$$\mathcal{B}(q_z, q_\perp) = \mathcal{B}_0 (1 + \zeta^2 q_\perp^2 + \eta^4 q_\perp^4). \quad (17)$$

All the other expansion terms either simply lead to a renormalization of K_1 (presumed to be small anyhow) or they do not add up to the convergence of the free energy.

This form immediately leads to a density-density correlation function in the (x, y) plane which oscillates and decays exponentially [15]. Specifically the correlation function $\mathcal{S}(\rho, z)$ averaged over the length of the polymers assumes the form

$$\frac{1}{L} \int_0^L S(\rho, z) = \frac{1}{4\pi\mathcal{B}_0\zeta^2} \left(\frac{\zeta}{\eta}\right)^4 * \text{Re} \left\{ \frac{K_0(u_1\rho/\zeta) - K_0(u_2\rho/\zeta)}{u_1^2 - u_2^2} \right\}, \quad (18)$$

where $u_{1,2}^2$ are the two complex zeros of $1 + u^2 + (\eta/\zeta)^4 u^4 = 0$, and $K_0(x)$ is the modified Bessel function. The form, Eq. (18), of the transverse correlation function is a reasonable ansatz for a liquid structure factor. Evaluating the integral [Eq. (11)] leads to the expression

$$\mathcal{F} = \mathcal{F}_0 + \frac{k_B T V}{16\sqrt{2}\pi} \sqrt[4]{\frac{\mathcal{B}_0}{K_3}} \zeta^{-5/2} \int_0^\infty \frac{u^{3/2} du}{[1 + u^2 + (\eta/\zeta)^4 u^4]^{3/4}}. \quad (19)$$

We essentially derived the same result as in Eq. (15). The only difference is that $q_{\perp\text{max}}$ has been replaced by ζ^{-1} . ζ represents the correlation length in a liquid, which for a typical liquid goes as the distance between next neighbors. Equation (19) suggests that instead of considering higher order terms we can simply choose a cutoff proportional to the Brillouin-zone radius $q_{\perp\text{max}} \approx \pi/d$, where d is the effective separation between the polymers in the nematic phase. This is a physically meaningful and appropriate cutoff because the underlying macroscopic elastic model has, by definition, to break down at wavelengths comparable to the distance between molecules.

Let us now see how our free energy scales for hard-core repulsion between chains. First we take the limit of low density $q_{\perp\text{max}} \ll 2\sqrt{\mathcal{B}K_3/K_1^2}$. For an elastic polymer K_3 has two additive terms, an intrinsic one and an interaction contribution. The first one stems from the elastic nature of the polymers themselves and has the form $K_3 \approx k_B T \mathcal{L}_p \rho_0$, while the second term is the generic form valid for any steric interaction with a hard core a , i.e., $K_3 \approx k_B T/a$ [16]. We now use the Helfrich self-consistent argument to evaluate the free energy due to elastic fluctuations in a hard-core potential. It amounts to taking $\mathcal{B} = V \partial^2 \mathcal{F} / \partial V^2$, where V is the volume of the system which can be taken as $V = L \times d^2$, L being the length of the sample. The crucial step is now to choose the cutoff which we set as $q_{\perp\text{max}} \approx \pi/d$. Inserting this into Eq. (15) and taking into account that the dominant behavior of K_3 will be $K_3 \approx k_B T \mathcal{L}_p \rho_0$, we remain with

$$\mathcal{F}(d) \sim L d^2 \sqrt[4]{\frac{d^4}{k_B T} \frac{\partial^2 \mathcal{F}(d)}{\partial (d^2)^2}} d^{-5/2}. \quad (20)$$

The solution of this differential equation leads to the scaling form for the fluctuation free energy, i.e., $\mathcal{F}(d) \sim d^{-2/3}$.

In the opposite limit we need to estimate K_1 , which is, following de Gennes and Prost [16], obtained as $K_1 \sim k_B T/a$, where a is the hard-core diameter of the polymers. Thus in this case we obtain

$$\mathcal{F}(d) \sim L d^2 \sqrt{\frac{d^2 a^2}{k_B T} \frac{\partial^2 \mathcal{F}(d)}{\partial (d^2)^2}} d^{-2}, \quad (21)$$

the solution of which leads to the scaling form $\mathcal{F}(d) \sim d^{-2}$. By analyzing whether $q_{\perp\text{max}}$ is smaller or larger than $2\sqrt{\mathcal{B}K_3/K_1^2}$ it is easy to ascertain that the first limiting law should be valid for larger and the latter for smaller relative densities of the polymers.

Interestingly we just derived the same scaling laws as those from corresponding mean-field models by Helfrich and Harbich [17] and de Gennes [18].

III. MEAN-FIELD MODELS

The mean-field theory that corresponds to our problem describes a single polymer in a liquid crystalline matrix. In this view the polymer fluctuates in the field of its neighbors. These mean-field models (one could also say ‘‘Einstein’’ cage models [19]) are strictly valid only for a hexagonal liquid crystal phase where the average position of a single polymer chain is well defined. In nematiclike phases the mean-square displacements are infinite and one has to choose a different language [Eq. (1)]. Although mean-field models are not the proper description for our problem, they still illustrate the underlying physics. We therefore review their results.

Let us imagine a flexible (elastic) polymer in a hard tube of diameter D , oriented on average along the axis of the tube, described with a Hamiltonian of a persistent chain [20]

$$\mathcal{H} = \frac{1}{2} k_B T \mathcal{L}_p \int ds \left(\frac{d^2 \mathbf{r}(s)}{ds^2} \right)^2, \quad (22)$$

where \mathcal{L}_p is the persistence length of the polymer, associated with its bending elastic constant $k_c = k_B T \mathcal{L}_p$. For small deviations away from the average polymer position along the z direction the two-dimensional (2D) displacement vector $\mathbf{r}(s)$ can be written as $\mathbf{r}(s) = (r_x(s), r_y(s))$. We assume that the diameter of the tube is small enough (smaller than the persistence length \mathcal{L}_p) so that between two consecutive hits with the walls of the tube, the polymer propagates ballistically,

$$\langle [\mathbf{r}(s) - \mathbf{r}(s')]^2 \rangle \approx \mathcal{L}_p (s - s')^2. \quad (23)$$

The longitudinal correlation length \mathcal{L}_{\parallel} can be obtained from evaluating the angle of the hit with the wall θ through statistics of a persistent chain, i.e.,

$$\theta^2 \approx \frac{D^2}{\mathcal{L}_{\parallel}^2} \sim \frac{\mathcal{L}_{\parallel}}{\mathcal{L}_p}, \quad \text{wherefrom } \mathcal{L}_{\parallel} \sim \mathcal{L}_p^{1/3} D^{2/3}. \quad (24)$$

The free energy corresponding to the bumping between the polymer and the wall on a length scale defined by \mathcal{L}_{\parallel} can thus be obtained as

$$\mathcal{F} \sim \frac{k_B T}{\mathcal{L}_{\parallel}} \sim D^{-2/3}. \quad (25)$$

This result has been obtained previously by Odijk [21] and Helfrich and Harbich [17] and represents a proper dimensional generalization of the Helfrich fluctuational force to 1D confined elastic objects.

On much larger length scales where the polymer chain effectively behaves as a free flight chain in two dimensions, the effect of local nematic order can be modeled through a simple nematic coupling term in the elastic energy of the type $[\mathbf{N}\mathbf{n}(s)]^2$ where \mathbf{N} is the average nematic director and $\mathbf{n}(s)$ is the local polymer director, i.e., $\mathbf{n}(s) = \dot{\mathbf{r}}(s)$. If \mathbf{N} is

directed again along the z axis, the dominant part of the chain Hamiltonian then assumes the form

$$\mathcal{H} = \frac{1}{2}g \int ds \left(\frac{d\mathbf{r}(s)}{ds} \right)^2, \quad (26)$$

where g gives the strength of the nematic coupling. This Hamiltonian gives rise to a diffusive propagation of the polymer chain described with

$$\langle [\mathbf{r}(s) - \mathbf{r}(s')]^2 \rangle \approx g^{-1}(s - s'), \quad (27)$$

if compared to the ballistic propagation of a persistent chain, Eq. (23). For too large deviations the effective tube again simulates the effects of steric interactions. The angle of the hit with the wall of the tube is obtained as

$$\theta^2 \approx \frac{D^2}{\mathcal{L}_{\parallel}^2} \sim \frac{1}{g\mathcal{L}_{\parallel}}, \quad \text{wherefrom } \mathcal{L}_{\parallel} \sim gD^2, \quad (28)$$

where we have now used the statistics of a free flight chain. The corresponding free energy is now obtained as

$$\mathcal{F} \sim \frac{k_B T}{\mathcal{L}_{\parallel}} \sim D^{-2}. \quad (29)$$

Both results have already been derived for confined polymers [18]. The point we wanted to make is that they are consistent with our macroscopic theory if the cutoff is chosen appropriately, meaning $q_{\perp \max} \approx d^{-1}$ while also equating the tube diameter D with the mean separation between the polymers d .

A similar approach can be used also in the case where confinement is not described by a short-range hard-core interaction but is mediated via a soft confinement potential of the form $V(\mathbf{r}(z))$. In this case, assuming that the fluctuations of the polymer position from its average are small, the Hamiltonian describing polymer elastic fluctuations can be written in the form

$$\begin{aligned} \mathcal{F} &= \frac{1}{2}k_c \int_0^L dz \left(\frac{d^2 \mathbf{r}(z)}{dz^2} \right)^2 + \int_0^L dz \tilde{V}(\mathbf{r}(z)) \\ &\approx \frac{1}{2}k_c \int_0^L dz \left(\frac{d^2 \mathbf{r}(z)}{dz^2} \right)^2 + \frac{1}{2}V'' \int_0^L dz \mathbf{r}^2(z), \end{aligned} \quad (30)$$

with

$$V'' = \nabla_{\perp}^2 \tilde{V}(\mathbf{r}(z)) = \left(\frac{1}{r} \frac{d\tilde{V}(\mathbf{r}(z))}{dr} + \frac{d^2 \tilde{V}(\mathbf{r}(z))}{dr^2} \right) \Bigg|_{r=D}, \quad (31)$$

where we have expanded the potential to second order in deviations from a straight line. One can define a length l^* analogous to the Odijk length by minimizing the energy with respect to the longitudinal size l of typical fluctuations [19]

$$\mathcal{F} \sim \frac{L}{l} \left(\frac{k_c r^2}{l^3} + V'' r^2 l \right) \rightarrow l^{*4} \sim \left(\frac{k_c}{V''} \right). \quad (32)$$

Thus we obtain for the confining energy

$$\mathcal{F}(D) \sim kT \frac{L}{l^*} \sim k_B T L \left(\frac{V''}{k_c} \right)^{1/4}, \quad (33)$$

which apparently depends on the fourth root of the confining potential stiffness V'' . This result is completely consistent with the one derived from a macroscopic theory, Eqs. (15), (16), in the limit $q_{\perp \max} \ll 2\sqrt{\mathcal{B}K_3/K_1^2}$, if we allow for the proper correspondence between the confining potential stiffness V'' and the isothermal compressibility modulus \mathcal{B} .

If, on the other hand, the polymer is presumed to be completely flexible with an orientational part of the potential energy described with a nematic coupling of the form Eq. (26), the Hamiltonian of a single confined chain will contain a softer elastic part proportional to $[d\mathbf{r}(s)/ds]^2$. In this case we have

$$\mathcal{F} = \frac{1}{2}g \int_0^L dz \left(\frac{d\mathbf{r}(z)}{dz} \right)^2 + \frac{1}{2}V'' \int_0^L dz \mathbf{r}^2(z), \quad (34)$$

where the confining potential stiffness has been defined in the same manner as before. Just as before we can again introduce the appropriate Odijk length l^* by minimizing the energy with respect to the longitudinal size l of typical fluctuations yielding [22]

$$\mathcal{F} \sim \frac{L}{l} \left(\frac{g r^2}{l} + V'' r^2 l \right) \rightarrow l^{*2} \sim \left(\frac{g}{V''} \right). \quad (35)$$

From here on by the same argument as before the confining energy scales as

$$\mathcal{F}(D) \sim kT \frac{L}{l^*} \sim k_B T L \left(\frac{V''}{g} \right)^{1/2}, \quad (36)$$

therefore as the square root of the confining potential stiffness. This result is now equivalent to the one derived from the macroscopic theory, Eqs. (15),(16), but this time in the limit $q_{\perp \max} \gg 2\sqrt{\mathcal{B}K_3/K_1^2}$.

To summarize, the mean-field theories surprisingly reproduce the same scaling laws under similar conditions (high and low density regimes) as our more detailed calculation from Sec. II. This indicates that the fluctuation part of the free energy is predominantly determined by the entropy loss of confining the polymer chains. Still, in order to model the free energy in more detail it is more appropriate to use our macroscopic model, because it predicts the correct cross-overs between the different regimes.

The mean-field approach with nematic coupling constant g as a free parameter, inferred from experiments, was used in [22] to argue that the effect of elastic fluctuations was to renormalize the decay length of underlying exponential repulsion. With the right choice of g , the calculated magnitude of the charge on DNA agrees reasonably with the numbers derived below and in Ref. [23]. Odijk [24] also proposed what amounts to a variation on the mean-field theme. It is based on a variational estimate for the Gaussian width of a single chain density distribution function. This theory in general does not lead to a straightforward renormalization of the decay length of the underlying soft exponential interactions

between chains. Also the phase boundaries calculated from this theory coupled to Lindemann's criterion [25] fall off the mark [26].

IV. MICROSCOPIC INTERACTIONS BETWEEN DNA MOLECULES

In order to use our main result [Eqs. (15),(16)] for the equation of state of nematic polymer liquid crystals we first have to guess how the macroscopic elastic constants K_1, K_2, K_3 and lateral compressibility \mathcal{B} depend on the density ($\rho_0 = 1/A = \sqrt{3}/d^2$ for hexagonally packed chains). Our first guess is the "one constant approximation" $K_1 = K_2 = K_3 \approx U(d)/d$ [16], where $U(d)$ is the interaction energy and d is the average distance between the molecules. In our case this approximation has to be modified, because the intrinsic bending stiffness k_c of the DNA molecules contributes additionally to the bending Frank constant K_3 .

$$K_1 = K_2 \approx U(d)/d,$$

$$K_3 \approx \rho_0 k_c + U(d)/d, \quad (37)$$

$$B \approx V \frac{\partial^2 \mathcal{F}_0(V)}{\partial V^2} = \frac{\sqrt{3}}{4L} \left(\frac{\partial^2 \mathcal{F}_0}{\partial^2 d} - \frac{1}{d} \frac{\partial \mathcal{F}_0}{\partial d} \right).$$

We now ask about the intermolecular interactions between two DNA molecules. There are two major contributions to the repulsion between DNA molecules in monovalent salt solutions [23]: (1) screened electrostatic repulsion from negative charges along the DNA backbone; (2) hydration repulsion coming from partially ordered water close to the DNA surface [27]. At the ionic strengths and polyelectrolyte densities considered in this work there appears to be no important contribution to the attractive part of the total DNA-DNA interaction: van der Waals forces are negligible [27] and counterion-correlation forces [28,29] are screened [30].

The mean-field electrostatic interaction is best described by the Poisson-Boltzmann theory resulting in an interaction potential between two parallel charged rods [31] of the form

$$U(d)/L = \frac{\xi^2}{2\pi\epsilon\epsilon_0} K_0(d/\lambda_D), \quad (38)$$

where λ_D is the Debye screening length. For ionic strengths I from monovalent salts, $\lambda_D = 3.08 \text{ \AA} / \sqrt{I[M]}$. Equation (38) refers to two infinitely thin line charges with a charge density per length ξ . This line-charge density is related to the actual surface charge density σ on a cylinder with radius a as follows:

$$\xi = 2\pi\sigma\lambda_D / K_1(a/\lambda_D). \quad (39)$$

For large d/λ_D the Bessel function K_0 can be approximated by

$$K_0(d/\lambda_D) \approx \sqrt{\frac{\pi}{2}} \frac{e^{-d/\lambda_D}}{\sqrt{d/\lambda_D}}. \quad (40)$$

The hydration repulsion between solvated molecules in water can be described by the same formalism as for screened electrostatic repulsion (see [32]). The interaction energy therefore goes as $K_0(d/\lambda_H)$ with $\lambda_H \approx 3 \text{ \AA}$ [23].

Knowing about the intermolecular interaction we can now revisit our main result, Eqs. (15),(16). From Eq. (37) it is clear that K_1 , K_2 , and the bulk compressibility modulus perpendicular to the chains \mathcal{B} essentially decay exponentially with d whereas K_3 after an initial exponential decay will at low densities be dominated by the intrinsic bending stiffness k_c of the polymers. This fact has instructive consequences. For lower densities, where we would expect fluctuations to be more prominent, only the limiting form valid for $q_{\perp \max} \ll 2\sqrt{\mathcal{B}K_3/K_1^2}$ remains. In this limit, using exponentially decaying interactions for \mathcal{B} , the fluctuation part of the free energy goes essentially as the fourth root of the direct interaction, since $K_3 = \rho_0 k_c$.

Summarizing, the bare interaction can be described in the following way (for simplicity we use the free energy per length $\mathcal{G} = \mathcal{F}/L$):

$$\mathcal{G}_0(d) = a \sqrt{\frac{\pi}{2}} \frac{e^{-d/\lambda_H}}{\sqrt{d/\lambda_H}} + b \sqrt{\frac{\pi}{2}} \frac{e^{-d/\lambda_D}}{\sqrt{d/\lambda_D}}, \quad (41)$$

where a and b are the amplitudes of the hydration and screened electrostatic repulsion. The total free energy \mathcal{G} , using the low density limit Eq. (15) using $q_{\perp \max} = \pi/d$, is then

$$\mathcal{G}(d) = \mathcal{G}_0(d) + k_B T \frac{(\pi)^{5/2}}{20\pi\sqrt{3}} k_c^{-1/4} \sqrt[4]{\frac{\partial^2 \mathcal{G}_0}{\partial^2 d} - \frac{1}{d} \frac{\partial \mathcal{G}_0}{\partial d}}. \quad (42)$$

V. MATERIALS AND METHODS

Sample preparation and determination of interaxial separations between DNA molecules by either x-ray or direct density measurements was described in detail previously [6].

At very low osmotic pressures (1/100 atm) the elasticity of the dialysis bags could contribute to osmotic pressure that acts on the sample. For this reason we performed experiments in which we dialysed low concentration (0.1–1 wt %) Dextran solutions against each other, to make sure that there were no residual osmotic pressures resulting from partially inflated dialysis tubes. After equilibration the Dextran concentrations inside and outside the dialysis bags agreed within 1% of the bathing concentration down to 0.1 wt % Dextran.

To compare our experimental results with our theory we expressed all data in terms of the interaxial spacing between two DNA molecules. Assuming hexagonal packing in all density regimes the relation between density and the interaxial spacing d is $\rho = (610/d[\text{\AA}])^2 [\text{mg/ml}]$.

The relation between the osmotic pressure Π and \mathcal{G} is then [27]

$$\frac{\partial \mathcal{G}}{\partial d} = \sqrt{3} \Pi d. \quad (43)$$

The nonlinear fits were done using the Levenberg-Marquardt method, implemented in the data analysis software Igor 3.03 (WaveMetrics, OR). The fit function used was [using \mathcal{G}_0 from Eq. (41)]

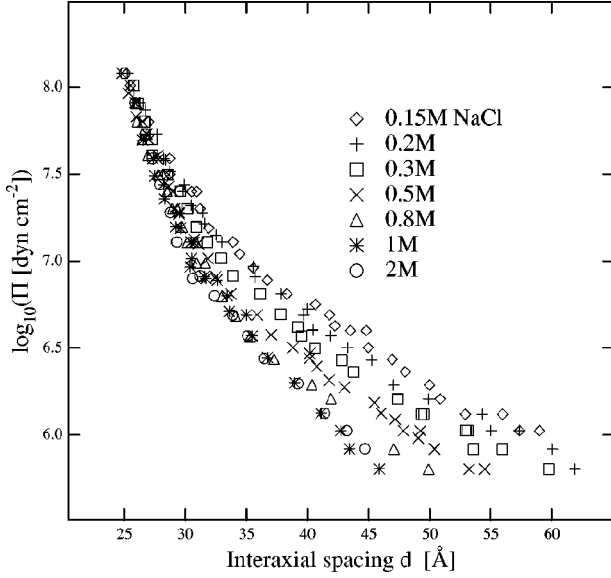


FIG. 2. Equation of state for DNA liquid crystals at ionic strength from $150mM$ to $2M$ NaCl. We plotted $\log_{10}\Pi$ versus interaxial spacing d . The interaxial spacing d was measured by x-ray scattering.

$$\frac{\partial \mathcal{G}}{\partial d} = \frac{\partial \mathcal{G}_0}{\partial d} + ck_B T k_c^{-1/4} \frac{\partial}{\partial d} \sqrt[4]{\frac{\partial^2 \mathcal{G}_0}{\partial^2 d} - \frac{1}{d} \frac{\partial \mathcal{G}_0}{\partial d}}, \quad (44)$$

where a and b are the bare amplitudes of the hydration and the screened electrostatic repulsion. Since the prefactor of the fluctuation part of the free energy depends on the cutoff wave vector we chose to fit it by the dimensionless constant c . The actual fit was performed using $\log_{10}(\partial \mathcal{G}/\partial d)$ versus interaxial spacing d . We did that to achieve an equal weight of all data points over the whole osmotic pressure regime.

VI. EXPERIMENTAL RESULTS

Figure 2 shows the equation of state ($\Pi-d$) for long DNA molecules at different NaCl concentrations ($10mM-2M$). The figure presents a compendium of data (from [27,23,33] and heretofore unpublished data) obtained up to date on the upper portion of the DNA phase diagram. At high osmotic pressures (Π) all ionic strengths merge into the same curve: an exponential decay with a decay length of about 3 \AA . We attribute this behavior to structural forces in water (hydration forces) commonly observed between hydrated surfaces in water [32]. At lower osmotic pressures the curves start to deviate from each other, reflecting the influence of screened electrostatic repulsion. Interestingly for ionic strengths $\geq 1M$ the curves are independent of ionic strength over the whole osmotic pressure regime. This indicates that for $I > 1M$ the electrostatic contributions are sufficiently screened so that the equation of state is dominated by hydration repulsion alone.

Figure 3 shows the measured $\partial \mathcal{G}/\partial d = \sqrt{3}\Pi d$ at $1M$ NaCl. Since from $1M$ on the electrostatic contribution is negligible we can use the data to determine the decay length of the hydration repulsion. We fitted the data according to Eq. (44) using only one exponentially decaying direct interaction. As fit parameters we used the amplitude of the hy-

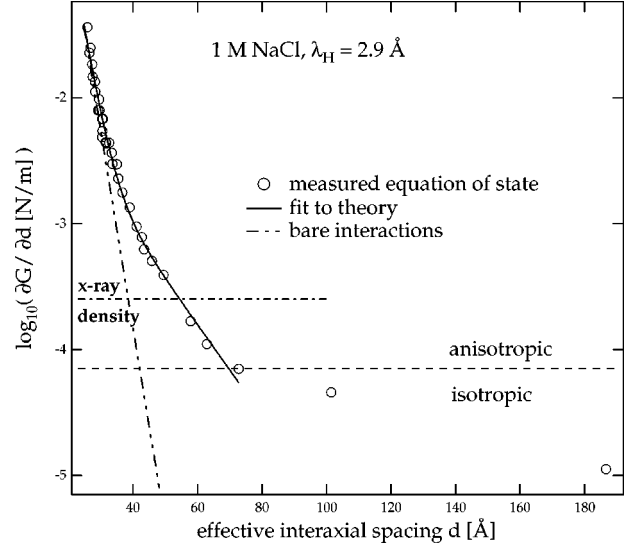


FIG. 3. Measured $\partial \mathcal{G}/\partial d$ for DNA liquid crystals at ionic strength of $1M$ over five orders of magnitude in osmotic pressure. The solid curve represents a fit of the data points in the anisotropic regime to a nematic liquid crystalline theory (see text) assuming exponential repulsion (hydration and screened electrostatics). The broken line represents the bare interaction without fluctuation enhanced repulsion. Interaxial spacings above the --- line are measured by x-ray scattering; below this line the spacings d are derived from measured DNA densities where molecules are expected to be hexagonally packed.

dration repulsion a , the hydration decay length λ_H , and the prefactor c of the fluctuation part of the free energy. The fit is shown as a solid line and describes the data very well. The resulting hydration decay length was $\lambda_H = (2.9 \pm 0.2) \text{ \AA}$. The amplitudes and the prefactor c are summarized in Table I.

Figures 4 and 5 show measured $\partial \mathcal{G}/\partial d$ for $0.5M$ and $0.1M$ NaCl. The solid line shown is the fit to Eq. (44) using a , b , and c as fit parameters. The hydration decay length was set to $\lambda_H = 2.88 \text{ \AA}$ and the Debye screening length was set to $\lambda_D = 3.08 \text{ \AA}/\sqrt{I[M]}$. The results are shown in Table I.

Figure 4 indicates the phase boundaries between the various liquid crystalline phases of DNA in detail. For all other salt concentrations we only indicated the isotropic to anisotropic transition. At very high osmotic pressures (not shown in Fig. 4) there exists a crystalline phase of DNA (see [34]). It melts into a line hexatic phase [regime (a)]: a three-dimensional liquid with long-range bond-orientational order perpendicular to the axis of the molecules [35]. As far as we can see, there is no indication for a hexagonal liquid crystalline phase in between the crystalline and the line hexatic phase. Between the line hexatic and the chiral phases of DNA the x-ray structure factor shows two peaks [regime (b)]: a sharper peak [continuing regime (a)] at smaller interaxial spacings and a more diffuse one at wider spacings [continued by regime (c)]. Since by using the osmotic stress method we hold all intensive variables (p, T, μ) fixed, the measured $S(q)$ should originate from a single phase (Gibb's phase rule). At this point it is not clear whether the structure in regime (b) corresponds to a new phase in between a line hexatic phase (nonchiral) and a cholesteric phase.

TABLE I. Summary of all fitted parameters for 1M, 0.5M, and 0.1M NaCl, as well as the corresponding line-charge density ξ , surface-charge density σ , and the fraction of unscreened phosphorus charges E .

I (M)	a (J/m)	λ_H (Å)	b (J/m)	λ_D (Å)	c	ξ (C/m)	σ (C/m ²)	E
1	$(1.7 \pm 0.9)10^{-7}$	(2.9 ± 0.2)		3.08	(1.2 ± 0.1)			
0.5	$(1.4 \pm 0.5)10^{-7}$	2.88	$(3 \pm 2.6)10^{-9}$	4.36	(1.3 ± 0.2)	2.1×10^{-9}	0.07	0.49
0.1	$(1.1 \pm 0.3)10^{-7}$	2.88	$(4.1 \pm 0.3)10^{-10}$	9.74	(0.8 ± 0.06)	7.8×10^{-10}	0.07	0.48

The chiral phases start with a cholesteric phase as observed by electron microscopy and polarization microscopy [36,37]. At even lower concentrations there is some indication for additional chiral phases (precholesteric phase [38] and blue phases [39]). Finally the anisotropic liquid crystalline phase melts into an isotropic phase [26] [regime (d)].

VII. DISCUSSION

DNA is highly charged (two negative charges per base-pair or 3.4 Å of its length). In an electrolyte solution the DNA's net negative charge creates an accumulation of counterions close to its surface that screen part of the bare charge and lead to an effective charge density that is felt at long distances between chains. Theoretically this effect can be captured by nonlinear Poisson-Boltzmann theory [40].

Even though our nematic polymer liquid crystalline theory was based on a rather simplistic model it describes all the data fairly well with reasonable values for the fitted parameters. In Table I we have summarized the corresponding line-charge densities and surface-charge densities that were calculated according to Eq. (38) and Eq. (39). At 0.5M and 0.1M the fits give the same surface-charge density $\sigma = 0.07 \text{ C/m}^2$. This value corresponds to about 50% of the bare charge of DNA (0.15 C/m^2).

Our result of 50% effective charge agrees very well with

the analysis of electrophoretic measurements [41] by Schellman and Stigter [42] that resulted in about 60% effective charge density for Na DNA. A recent study using steady-state electrophoresis reported 10% for Na DNA [43]. This discrepancy exists not because of experimental uncertainty, but because of different theoretical treatments of the measured mobilities (for a recent discussion see [44]). Part of the difference might come from the complicated details of frictional forces acting on a rough, charged polyelectrolyte.

One has to bear in mind that for the 0.5M data the uncertainty of the fitted amplitude is almost 100%. This uncertainty is not very surprising considering the close proximity of the two decay lengths $\lambda_H = 2.9 \text{ Å}$ and $\lambda_D = 4.36 \text{ Å}$. As soon as the decay lengths separate from each other, as in the case for 0.1M, the statistical uncertainty drops to 10%.

We also fitted the prefactor c . If in the theory [Eq. (42)] one chooses the cutoff wave vector to be at the Brillouin-zone radius $q_{\perp \text{max}} = \pi/d$, the prefactor c is $\pi^{3/2}/20\sqrt{3} = 0.16$. The fitted prefactors c [Eq. (44)] range from 1.3 to 0.8. This is about 5–8 times larger than the theory predicted. On the other hand, considering the simple underlying model, the value is not too far off. Choosing a cutoff at twice the Brillouin-zone radius, for example, would give a value right on the fitted one. In our view, the prefactor depends on the fine details of the in-plane structure factor $S(q_{\perp})$ [see Eq. (19)]. In the case of exponential direct interactions between the chains any algebraic dependence of the cutoff with respect to the density will be dominated by the fourth root of the direct interaction [Eq. (42)]. The fact that for different

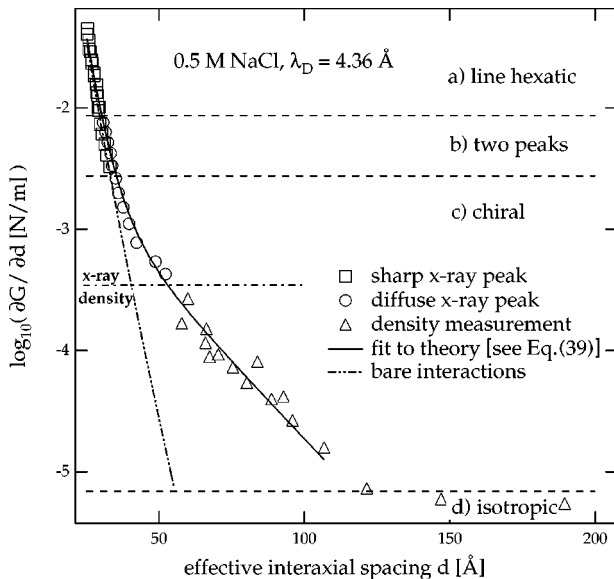


FIG. 4. Measured $\partial G/\partial d$ for DNA liquid crystals at ionic strength of 0.5M over five orders of magnitude in osmotic pressure. Four structural regimes (a)–(d) could be distinguished. See Fig. 3 for annotations.

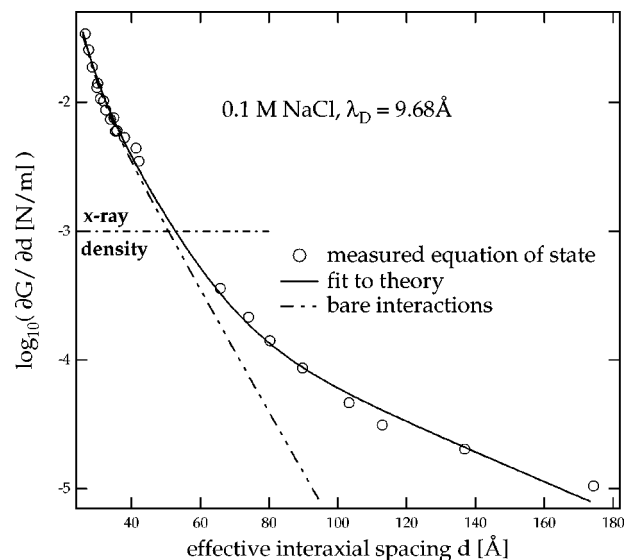


FIG. 5. Measured $\partial G/\partial d$ for DNA liquid crystals at ionic strength of 0.1M. See Fig. 3 for annotations.

ionic strength the prefactors have similar values (all around 1) strengthens our argument.

The fits even seem to prove explicitly the presence of hydration repulsion. If one tries to calculate the charge densities for 1M, using a screening length of $\lambda_D = 3.08 \text{ \AA}$ and ignoring any contribution of hydration repulsion, the surface-charge density results in $\sigma = 0.19 \text{ C/m}^2$, 25% more charge than the total phosphorus charges on DNA. Since it is generally believed that more than half of the bare charge on DNA is screened, a picture with pure electrostatic double layer repulsion is hard to envision. Recently Lyubartsev and Nordenskiöld [45] published a Monte Carlo simulation addressing the DNA case, comparing their results with osmotic stress measurements from our laboratory. They showed that electrostatic repulsion strongly increased beyond simple linearized Poisson-Boltzmann theory, when two charged cylinders approach each other closely. However, this simulation used a solid cylinder model of DNA and hard-sphere $d = 4 \text{ \AA}$ ions. The measurements are in a regime where most of the aqueous volume is inside the DNA grooves rather than outside any DNA cylinder. Better models have to include the possibility of ions entering the groove space. Although their results seem to fit the data for 0.5M quite well, there is not as good success at other salt concentrations. We take the force data in high salt concentration to be strong evidence for hydration repulsion. Even noncharged polymers, like the polysaccharide schizophyllan, show an exponentially decaying repulsion with a decay length of about $\lambda_H = 3.4 \text{ \AA}$ [46]. Hydration repulsion is a general feature of water soluble molecules at separations $\leq 1 \text{ nm}$ [32] that cannot be simply denied [47].

Osmotic stress measurements can be used to determine more directly effective charge densities of semiflexible polyelectrolytes. We can therefore test and compare theories that predict effective charge densities, like nonlinear Poisson-Boltzmann or Manning theory [48]. Our results indicate that for Na the effective charge is twice as large as predicted by both theories. Previous studies in our laboratory [23] observed significant differences in charge densities using different counterions, such as Li, Na, K, Cs, and Tri-methylammonium. These results merit further analysis.

The form of the fluctuation part of the free energy [Eq. (42)] suggests that fluctuation enhanced repulsion may be important for many lyotropic polymer liquid crystalline systems. The prefactor c of the fluctuation part only depends weakly on the bending constant of the polymer $c \propto k_c^{-1/4}$. The only condition for enhanced repulsion is that the polymers are longer than their persistence length, and that they remain in a nematiclike phase.

Another appealing conclusion from our work is the emerging connection between multilamellar lipid and columnar polyelectrolyte (DNA) arrays. Both are governed by the same type of colloidal forces [49], except that for polyelectrolyte arrays the attractive forces at relevant ionic strengths and polymer concentrations are usually negligible, and show the same conformational flexibility describable by an elastic term in the conformational Hamiltonian (Helfrich [50] in the case of lipid multilayers and Kratky-Porod [20] in the case of semiflexible chains). The interplay between fluctuations and effective interaction in multilamellar arrays has been a topic

for quite awhile [51] and is at present reasonably well understood.

Setting aside the attractive part in the bare interaction potential and the different dimensionality of the fundamental interacting objects (2D in the case of lipid multilayers vs 1D in the case of polyelectrolytes), multilamellar lipid and columnar polyelectrolyte arrays share exactly the same Hamiltonian. This leads to the same type of fluctuational renormalization of interaction force that can be expressed by the following two forms of free energy:

$$\mathcal{F} \approx \frac{k_B T V}{5 \times 2^{3/2} \pi} \sqrt[4]{\frac{\mathcal{B}}{K_3}} q_{\perp \max}^{5/2} + \dots$$

$$\text{vs } \mathcal{F} \approx \frac{k_B T V}{16 \pi} \sqrt{\frac{\mathcal{B}}{K_3}} q_{\perp \max}^2 + \dots \quad (45)$$

The first one pertains to the fluctuations in polyelectrolyte arrays, cf. Eq. (16), and the second one to the fluctuations in multilamellar systems, e.g., [52]. Both these results are written in the limit of small density of fluctuating objects. The apparent formal differences between the two expressions are due *solely* to the dimensional difference between the fluctuating objects, i.e., 1D as opposed to 2D.

The main difference between multilamellar and columnar arrays interacting through exponential repulsive forces would thus be the twofold vs fourfold renormalization of the decay length.

There have recently (see [53] for an overview), and maybe not so recently [54], appeared quite a few speculations on the possible attractive component to the polyelectrolyte interaction forces. At polyelectrolyte densities and ionic strengths described in this work, there is certainly no evidence to presume there are any. We cannot, however, exclude the possibility that low ionic strengths and low polyelectrolyte densities, thus promoting pronounced unscreened counterion fluctuations [55,30], conspire to bring forth non-negligible attractive forces between DNA molecules. Should this turn out to be the case, columnar polyelectrolyte arrays would become even more similar to multilamellar lipid arrays. DNA and cell membranes are among the principal organizational structures in biology. That they share such a pronounced amount of common physics certainly adds up to a rather pleasing intellectual development.

ACKNOWLEDGMENTS

We want to thank Don Rau, David Nelson, Robijn Bruinsma, and Per Lyngs Hansen for fruitful discussions, and Gary Melvin and Leepo Yu for their support, enabling the x-ray experiments. Special thanks are due to Randy Kamien for many delightful discussions and valuable comments. We would like to thank the Aspen Institute for Physics for their hospitality during the workshop on ‘‘Topological Defects in Condensed Matter Physics.’’

- [1] F. Livolant and Y. Bouligand, *J. Phys. (France)* **47**, 1813 (1986).
- [2] F. Livolant, *Physica A* **176**, 117 (1991).
- [3] F. P. Booy, W. W. Newcomb, B. L. Trus, J. C. Brown, T. S. Baker, and A. C. Steven, *Cell* **64**, 1007 (1991).
- [4] T. Strzelecka, M. Davidson, and R. Rill, *Nature (London)* **331**, 457 (1988).
- [5] A. Wolffe, *Chromatin, Structure and Function* (Academic Press, San Diego, 1992).
- [6] H. H. Strey, V. Parsegian, and R. Podgornik, *Phys. Rev. Lett.* **78**, 895 (1997).
- [7] V. A. Parsegian, R. P. Rand, N. L. Fuller, and D. C. Rau, *Methods Enzymol.* **127**, 400 (1986).
- [8] P. de Gennes, *Mol. Cryst. Liq. Cryst. Lett.* **34**, 177 (1977).
- [9] R. Meyer, in *Polymer Liquid Crystals*, edited by A. Ciferri, W. Krigbaum, and R. Meyer (Academic, New York, 1982), p. 133.
- [10] R. D. Kamien and J. Toner, *Phys. Rev. Lett.* **74**, 3181 (1995).
- [11] A. Semenov and A. Kokhlov, *Usp. Fiz. Nauk* **156**, 427 (1988) [*Sov. Phys. Usp.* **31**, 988 (1988)].
- [12] P. Le Doussal and D. R. Nelson, *Europhys. Lett.* **15**, 161 (1991).
- [13] R. D. Kamien, P. Doussal, and D. Nelson, *Phys. Rev. A* **45**, 8727 (1992).
- [14] J. Selinger and R. Bruinsma, *Phys. Rev. A* **43**, 2910 (1991).
- [15] D. Zubarev, *Nonequilibrium Statistical Thermodynamics* (Plenum, New York, 1974).
- [16] P. de Gennes and J. Prost, *The Physics of Liquid Crystals*, 2nd ed. (Oxford University Press, Oxford, 1993).
- [17] W. Helfrich and W. Harbhich, *Chem. Scr.* **25**, 32 (1985).
- [18] P. de Gennes, *Scaling Concepts in Polymer Physics* (Cornell University Press, Ithaca, 1979).
- [19] S. Jain and D. Nelson, *Macromolecules* **29**, 8523 (1996).
- [20] O. Kratky and G. Porod, *Recl. Trav. Chim. Pays-Bas.* **68**, 1106 (1949).
- [21] T. Odijk, *Macromolecules* **19**, 2313 (1986).
- [22] R. Podgornik and V. Parsegian, *Macromolecules* **23**, 2265 (1990).
- [23] R. Podgornik, D. Rau, and V. Parsegian, *Biophys. J.* **66**, 962 (1994).
- [24] T. Odijk, *Biophys. Chem.* **46**, 69 (1993).
- [25] T. Odijk, *Europhys. Lett.* **24**, 177 (1993).
- [26] K. Merchant and R. L. Rill, *Biophys. J.* **73**, 3154 (1997).
- [27] D. Rau, B. Lee, and V. Parsegian, *Proc. Natl. Acad. Sci. USA* **81**, 2621 (1984).
- [28] F. Ossawa, *Polyelectrolytes* (Marcel Dekker, New York, 1971).
- [29] J.-L. Barrat and J.-F. Joanny, in *Advances in Chemical Physics*, edited by I. Prigogine and S. Rice (John Wiley & Sons, New York, 1995), Vol. 94, pp. 1–66.
- [30] R. Podgornik and V. Parsegian, *Phys. Rev. Lett.* **80**, 1560 (1997).
- [31] S. Brenner and V. Parsegian, *Biophys. J.* **14**, 327 (1974).
- [32] S. Leikin, V. Parsegian, D. Rau, and R. Rand, *Annu. Rev. Phys. Chem.* **44**, 369 (1993).
- [33] R. Podgornik, D. Rau, and V. Parsegian, *Macromolecules* **22**, 1780 (1989).
- [34] R. Langridge, H. R. Wilson, C. W. Hooper, M. H. F. Wilkins, and L. D. Hamilton, *J. Mol. Biol.* **2**, 19 (1960).
- [35] R. Podgornik, H. H. Strey, K. Gawrisch, D. C. Rau, A. Rupprecht, and V. A. Parsegian, *Proc. Natl. Acad. Sci. USA* **93**, 4261 (1996).
- [36] A. Leforestier and F. Livolant, *Biophys. J.* **65**, 56 (1993).
- [37] R. Podgornik, H. Strey, D. Rau, and V. Parsegian, *Biophys. Chem.* **57**, 111 (1995).
- [38] F. Livolant, *J. Phys. (France)* **48**, 1051 (1987).
- [39] A. Leforestier and F. Livolant, *Liq. Cryst.* **17**, 651 (1994).
- [40] D. Stigter, *Biophys. J.* **69**, 380 (1995).
- [41] P. Ross and R. Scruggs, *Biopolymers* **2**, 231 (1964).
- [42] J. Schellman and D. Stigter, *Biopolymers* **16**, 1415 (1977).
- [43] T. M. Laue, T. M. Ridgeway, J. O. Wooll, H. K. Shepard, T. P. Moody, T. J. Wilson, J. B. Chaires, and D. A. Stevenson, *J. Pharm. Sci.* **85**, 1331 (1996).
- [44] D. A. Hoagland, D. L. Smisek, and D. Y. Chen, *Electrophoresis* **17**, 1151 (1996).
- [45] A. Lyubartsev and L. Nordenskiöld, *J. Phys. Chem.* **99**, 10373 (1995).
- [46] D. C. Rau and V. A. Parsegian, *Science* **249**, 1278 (1990).
- [47] J. Israelachvili and H. Wennerström, *Nature (London)* **379**, 219 (1996).
- [48] G. Manning, *Q. Rev. Biophys.* **11**, 179 (1978).
- [49] V. Parsegian and E. Evans, *Curr. Opin. Colloid Interface Sci.* **1**, 53 (1996).
- [50] W. Helfrich, *Z. Naturforsch. C* **28**, 693 (1973).
- [51] *Structure and Dynamics of Membranes*, Handbook of Biological Physics Vol. 1, edited by R. Lipowsky and E. Sackmann (Elsevier Science B.V., Amsterdam, 1995).
- [52] W. Helfrich, *Z. Naturforsch. A* **33A**, 305 (1978).
- [53] K. Schmitz, *Macroions in Solution and Colloidal Suspensions* (VCH Publishers, New York, 1993).
- [54] I. Sogami and N. Ise, *J. Chem. Phys.* **81**, 6320 (1984).
- [55] N. Gronbech-Jensen, R. Mashi, R. Bruinsma, and W. Gelbart, *Phys. Rev. Lett.* **78**, 2477 (1997).